Boosting Capacity for 6G Terahertz Mesh Networks Based on Bottleneck Structures

Tianxin Wang and Xudong Wang
Shanghai Jiao Tong University, Shanghai, China 200240
Email: tianxin.wang@sjtu.edu.cn, wxudong@ieee.org

GLOBECOM 2023 - 2023 IEEE Global Communications Conference | 979-8-3503-1090-0/23/$31.00 ©2023 IEEE | DOI: 10.1109/GLOBECOM54140.2023.10436964

***Abstract*—Terahertz (THz) mesh networking is envisioned as a promising technology for 6G networks, with network capacity as one of the most critical performance metrics. To boost the network capacity of a THz mesh network, link resource planning is conducted, which poses two challenges. First, the relationship between link resources and network capacity must be captured quantitatively considering the peculiarities of THz mesh networking. Second, multi-dimensional resources including subarrays, power, and subbands need to be determined for link resource planning. To address the first challenge, a bottleneck structure is constructed by adapting the quantitative theory of bottleneck structures in the recent work [1] for THz mesh networks, such that the relationship between network capacity and a certain link resource planning result is determined. Furthermore, bottleneck gradients are computed based on the constructed bottleneck structure. Given the derived relationship and bottleneck gradients, a heuristic link resource planning algorithm is designed to allocate multi-dimensional resources, thus resolving the second challenge. Performance results show that the heuristic resource planning algorithm can boost the network capacity by $20.3\% - 41.8\%$ for various topologies.**

***Index Terms*—quantitative theory of bottleneck structures, terahertz mesh networks, network capacity, link resource planning.**

I. Introduction

To satisfy the demand of multi-gigabit-per-second and even terabit-per-second data rates, terahertz band (THz, 0.1-10 THz) is envisioned as a critical band with rich frequency resources for future 6G networks [2]. However, THz networking is faced with many challenges. Particularly, THz links suffer from huge path loss and severe blockage issues. To increase transmission distances and alleviate link blockage issues, THz mesh networking enabled by multi-hop directional links is a promising technology [3]. For 6G THz mesh networks, one of the most critical performance metrics is network capacity, which in this paper is characterized by network saturation throughput under the given end-to-end flow distribution.

Achieving high network capacity in multi-hop networks is a fundamental challenging problem. As shown in Fig. 1, in a THz mesh backhaul network, network congestion happens when links are overloaded with packet traffic, and network bottlenecks are formed in different regions, which negatively impacts the overall network capacity. To boost capacity of the entire THz mesh network, network congestion needs to be alleviated, and bottlenecks need to be resolved. Existing work on addressing network congestion is categorized into two lines of work. The first line is rate control [4], where source rates of flows are dynamically adjusted to avoid congestion. In this case, network capacity is sacrificed for alleviating congestion. Another line of work is load balancing [5], where the traffic load of a link is viewed as one of the routing metrics. With load balancing, new routes are determined by circumventing those heavily-loaded bottleneck links. These new load-balanced routes may go through more hops than the original routes. Although congestion can be alleviated by load balancing, the overall network capacity may not be increased by a large margin.

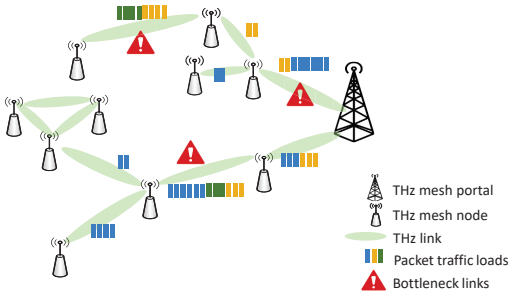


Fig. 1. THz mesh backhaul networks.

In the face of the above situation, ***link resource planning*** is considered as an effective approach to boosting network capacity, where link capacities are adjusted by planning antennas, subbands, and power based on the distribution of bottlenecks in the network. As compared with the traditional resource allocation scheme [3], link resource planning is distinct with the capability of resolving network bottlenecks via planning link resources, which is conducted on a large timescale. It is noted that both rate control and load balancing can be applied on top of link resource planning to further alleviate congestion. In contrast to link resource planning, topology planning boosts network capacity by obtaining a new topology that contains more and better end-to-end transmission paths, which leads to another research topic independent of link resource planning. This work is focused on link resource planning for a THz mesh network with a fixed topology, such as a backhaul network.

To conduct link resource planning, challenges lie in two aspects. First, the relationship between link resources and network capacity must be quantitatively determined for THz mesh networks, which specifies how link resource planning affects the formation of network bottlenecks and how these formed

The research was sponsored by Huawei Research Fund TC20210621023, and also by the National Natural Science Foundation of China (NSFC) under Grant No. 62371292.

Authorized licensed use limited to: University of Edinburgh. Downloaded on October 18,2026 at 20:09:29 UTC from IEEE Xplore. Restrictions apply.

bottlenecks interact with each other. This relationship needs to capture the peculiarities of THz mesh networking such as highly directional transmission and channel characteristics. Second, given the derived relationship, multi-dimensional resources including antennas, power, and subbands need to be determined for link resource planning, with the objective of maximizing network capacity.

To address the first challenge, the quantitative theory of bottleneck structures (QTBS) developed in the recent work [1] is adapted for THz mesh networks to derive the relationship between network capacity and link resources. This relationship is implicitly captured by the construction of a bottleneck structure, as specified in Section III-D. QTBS is also named the ***bottleneck theory*** in the rest of the paper for simplicity. Although the bottleneck theory is originally leveraged for data center networks [1], it is tailored for THz mesh networks by considering the peculiarities of THz mesh networking, as elaborated in Section II. To address the second challenge, bottleneck gradients are first computed based on the constructed bottleneck structure to quantify how the capacity increase of each bottleneck link impacts the overall network capacity. Next, a heuristic algorithm for multi-dimensional link resource planning is designed, where bottleneck structure construction and link resource planning are iteratively conducted until convergence. For link resource planning in each iteration, the links with larger bottleneck gradients are favored with more resources. As a result, network capacity is significantly boosted by the ultimate link resource planning result.

The main contributions of this paper are summarized as follows:

- Leveraging the bottleneck theory, a bottleneck structure is constructed to determine the relationship between link resources and network capacity by considering the peculiarities of THz mesh networking.
- Bottleneck gradients are determined to quantify how the capacity increase of each bottleneck link impacts the overall network capacity based on the constructed bottleneck structure.
- A heuristic algorithm is designed to plan multi-dimensional link resources based on the determined relationship and bottleneck gradients. This algorithm significantly boosts network capacity compared with baseline methods.

The rest of the paper is organized as follows. In Section II, motivation and system model are presented. The link resource planning problem is stated in Section III. Afterwards, the design framework and detailed algorithm are also elaborated in Section III. Performance evaluation is conducted in Section IV, and the paper is concluded in Section V.

II. Motivation and System Model

A. Motivation

The bottleneck theory is originally proposed in [1], and utilized for capacity planning in data center networks [6]. The key idea of the bottleneck theory is to construct a bottleneck structure, i.e., a directed acyclic graph (DAG), to capture the interactions among the formation of multiple bottlenecks given link capacities and flow distribution, through which network saturation throughput is obtained. The detailed description of bottleneck structures is in Section III-D.

A THz mesh network is considered to be a near-wired network when it possesses the following three features. First, due to highly directional transmission, cross-link interference (or inter-beam interference) is significantly suppressed, and thus most of the links in the network can reuse radio resources. Second, at each network node, multiple directional beams are formed concurrently enabled by hybrid beamforming [7]. Third, frequency division duplex (FDD) mode is adopted for each network node, and thus transmitting and receiving beams can be activated at the same time. This paper is focused on the THz mesh network with the above three features, and the existing bottleneck theory is adapted for this type of network.

Based on the bottleneck theory, we aim to conduct link resource planning in THz mesh networks. There exist two key differences than the wired case. First, link resource planning in THz mesh networks is constrained by the given system bandwidth, power, and antenna resources, and link capacities are also subject to THz channel conditions. Second, as inter-beam interference cannot be completely ignored, it is necessary to suppress the interference to guarantee the required SINR when each link's multi-dimensional resources are determined.

B. Network Set-up

A FDD-based THz mesh backhaul network with a fixed topology is considered, which consists of one mesh portal and multiple mesh nodes. As shown in Fig. 1, the mesh portal conducts centralized link resource planning on a large time-scale [8]. Network nodes (the mesh portal and mesh nodes) communicate with each other via highly directional links. There are F end-to-end multi-hop flows (denoted by $\mathcal{F}$) carried by the network. In the backhaul network, each flow aggregates traffic on the access links, and hence it is termed as an aggregated flow, which remains stable on a large timescale. Given an aggregated flow between any pair of nodes, single-path routing is adopted. Let $\mathcal{D} = \{\mathcal{R}_1, ..., \mathcal{R}_F\}$ be the set of routes with $\mathcal{R}_f$ as flow f's routes. $\mathcal{D}$ is also referred to as flow distribution which remains unchanged during link resource planning. Let $\mathcal{N}$, $\mathcal{L}$, $\mathcal{K}$ be the set of network nodes, directed links, and available subbands respectively. Let n, l, k be the index of a network node, a directed link, and a subband.

C. THz Channel and Beamforming Models

The Saleh-Valenzuela (S-V) model [9] is adopted. Assuming link l is equipped with N_l^{t} antennas at the transmitter and N_l^{r} at the receiver, let $\mathbf{H}_{l,k} \in \mathbb{C}^{N_l^{\mathrm{r}} \times N_l^{\mathrm{t}}}$ denote the THz MIMO channel matrix at subband k for link l, which follows the expression in [9]. Each node is deployed with a a array-of-subarray hybrid beamforming architecture. Power and antenna constraints are imposed on each node n with total transmit power P and M subarrays (with $M/2$ for transmitting and receiving links respectively). Multi-beam-based transmission

Authorized licensed use limited to: University of Edinburgh. Downloaded on October 18,2026 at 20:09:29 UTC from IEEE Xplore. Restrictions apply.

is enabled by hybrid beamforming [7], where each beam only serves one link with A_l^{t} and A_l^{r} as the number of subarrays at its transmitting and receiving nodes respectively. Let $N_l^{\mathrm{t}} = A_l^{\mathrm{t}} N_{\mathrm{sa}}$ and $N_l^{\mathrm{r}} = A_l^{\mathrm{r}} N_{\mathrm{sa}}$, with N_{sa} as the number of antennas in each subarray. The optimal analog and digital beamforming vectors are assumed to be obtained via existing methods [9]. Due to the sparsity of THz channels, only a single data stream is considered [7]. The effective channel gain $h_{l,k}^{\mathrm{eff}}$ is

$$h_{l,k}^{\mathrm{eff}} = \mathbf{V}_{l,k}^{\mathrm{T}} \mathbf{H}_{l,k} \mathbf{W}_{l,k}, \tag{1}$$

where $\mathbf{W}_{l,k} \in \mathbb{C}^{N_l^{\mathrm{t}} \times N_l^{\mathrm{t}}}$ and $\mathbf{V}_{l,k} \in \mathbb{C}^{N_l^{\mathrm{r}} \times N_l^{\mathrm{r}}}$ are precoding and combining matrices respectively. With respect to inter-beam interference, the effective interfering channel from link m's transmitter to link l's receiver on subband k is denoted by $g_{m,l,k}^{\mathrm{eff}}$, which is $g_{m,l,k}^{\mathrm{eff}} = \mathbf{V}_{l,k}^{\mathrm{T}} \mathbf{G}_{m,l,k} \mathbf{W}_{m,k}$, where $\mathbf{G}_{m,l,k}$ is interfering MIMO channel from link m's transmitter to link l's receiver on subband k. Therefore, SINR at link l 's receiver on subband k is

$$\gamma_{l,k} = \frac{p_{l,k} |h_{l,k}^{\mathrm{eff}}|^2}{W N_0 + \sum_{m \in \mathcal{L} \setminus \{l\}} p_{m,k} |g_{m,l,k}^{\mathrm{eff}}|^2}, \tag{2}$$

letting $p_{l,k}$ denote the transmit power allocated to link l on subband k, and W denote the bandwidth of one subband.

III. Link Resource Planning Based on the Bottleneck Theory

In this section, the link resource planning problem is first stated in III-A: multi-dimensional resources including subarrays, subbands, and power are planned for each link, such that the network saturation throughput determined by the bottleneck theory is maximized. Next, the design framework of a heuristic approach is shown III-B. Three critical modules of the framework are designed in Section III-C, III-D, III-E, and the overall algorithm is summarized in Section III-F.

A. Problem Statement

The relationship between link capacities $\mathbf{C}$ and network saturation throughput T given the flow distribution is specified via a function $\mathcal{T} : (\mathbf{C}, \mathcal{D}) \rightarrow T$, where $\mathbf{C} = [C_1, ..., C_L]$ is the vector of link capacities and $\mathcal{D}$ is the flow distribution. This function is implicitly captured by the construction of a bottleneck structure in [10]. For THz mesh networks, this relationship is adapted by considering subarray, subband, and power planning, which is

$$T = \mathcal{T}(\mathbf{P}, \mathbf{B}, \mathbf{A}, \mathcal{D}), \tag{3}$$

where $\mathbf{P}$ is the power allocation matrix consisting of $p_{l,k}$, and $\mathbf{B}$ is the subband allocation matrix with its elements $b_{l,k}$, and $\mathbf{A}$ is the subarray allocation matrix consisting of A_l^{t} and A_l^{r}. Note that link l's capacity C_l is determined based on its subarray, power, and subband planning, expressed as

$$C_l = W \sum_{k \in \mathcal{K}} b_{l,k} \left[1 + \log_2 \gamma_{l,k}\right], \forall l \in \mathcal{L}, \tag{4}$$

where $b_{l,k}$ is binary subband allocation indicator ($b_{l,k} = 1$ means subband k is allocated to link l).

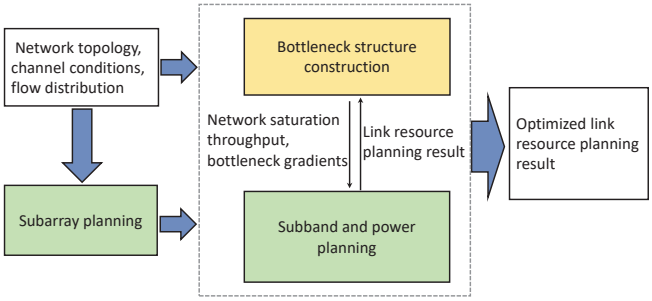


Fig. 2. Design framework.

Given the above relationship between network saturation throughput T and a certain link resource planning results, $\mathbf{P}, \mathbf{B}$, and $\mathbf{A}$ are optimized to maximize T while several principles must be followed. First, SINR of each link on its allocated subbands is guaranteed to be higher than the predetermined threshold γ_{th}, which is

$$b_{l,k} \gamma_{l,k} \geq b_{l,k} \gamma_{\mathrm{th}}, \forall l \in \mathcal{L}, k \in \mathcal{K}. \tag{5}$$

Second, as FDD is adopted, the transmitting and receiving links at each node must use orthogonal bands. Hence,

$$b_{l,k} + b_{m,k} \leq 1, \forall l \in \mathcal{L}_n^{\mathrm{t}}, m \in \mathcal{L}_n^{\mathrm{r}}, n \in \mathcal{N}, k \in \mathcal{K}, \tag{6}$$

where the links related to network node n are classified into two sets $\mathcal{L}_n^{\mathrm{t}}$ and $\mathcal{L}_n^{\mathrm{r}}$, representing transmitting link set and receiving link set respectively. Third, power planning must not exceed the total transmit power available at each network node, and the transmit power is non-negative, expressed by

$$\sum_{l \in \mathcal{L}_n^{\mathrm{t}}} \sum_{k \in \mathcal{K}} p_{l,k} \leq P, \forall n \in \mathcal{N}, \tag{7}$$

$$p_{l,k} \geq 0, \forall l \in \mathcal{L}, k \in \mathcal{K}. \tag{8}$$

Furthermore, subarray planning must not exceed the total number of subarrays at each network node, and A_l^{r}, A_l^{t} should be non-negative integers.

B. Design Framework

As shown in Fig. 2, the network topology, channel conditions, and flow distribution are collected as the inputs of our approach. Subarray allocation is conducted only for once in the beginning of resource planning, which is decoupled from subband and power planning. The main module is an iterative process between bottleneck structure generation and resource planning for subband and power. The bottleneck structure is generated given a certain subband and power planning result, and the bottleneck gradients and network saturation throughput obtained from the bottleneck structure are leveraged for the next iteration of subband and power planning. As a result, the optimized link resource planning result is obtained, based on which an optimized bottleneck structure can be constructed.

C. Subarray Allocation

Subarray allocation is conducted at each network node for its transmitting and receiving links separately. Note that

Authorized licensed use limited to: University of Edinburgh. Downloaded on October 18,2026 at 20:09:29 UTC from IEEE Xplore. Restrictions apply.

only the links with flows on them are considered. For the transmitting links of node n, the main-lobe beam gain is controlled to be much larger than the side-lobe beam gain, to suppress interference to the neighboring nodes of node n. $\beta \in (0,1)$ is selected as the pre-determined ratio of side-lobe to main-lobe beam gain. With the main-lobe beam gain normalized to 1, the side-lobe beam gain [11] of link l is required to satisfy

$$|G_l(\psi)|^2 = \frac{\sin^2(N_l^{\mathrm{t}}\frac{\psi}{2})}{N_l^{\mathrm{t}}\sin^2(\frac{\psi}{2})} \leq \beta \left|\frac{\mathrm{PL}(d)}{\mathrm{PL}(d')}\right|^2, \forall l \in \mathcal{L}_n^{\mathrm{t}}, \quad (9)$$

where $\psi = \frac{2\pi d}{\lambda}(\sin\theta - \sin\theta_l)$ is the deviation angle expressed in the ψ-space [12], with θ_l as link l's main lobe direction and θ as AoD of the node n's neighboring node. Specifically, the angle and distance information of neighboring nodes can be estimated and collected [7]. Since the distance d from link l's source (i.e., node n) to destination node can differ from the distance d' from node n to any neighboring node of node n, different path losses $\mathrm{PL}(d)$ and $\mathrm{PL}(d')$ are considered for main-lobe and side-lobe transmission in (9).

The minimum required number of transmit antennas $N_{l,\min}^{\mathrm{t}}$ is determined by satisfying (9) for all the neighboring nodes of node n. Due to large channel attenuation in THz bands, only one-hop and two-hop neighboring nodes are considered [13]. Thus, the number of transmit subarrays allocated to link l is $A_l^{\mathrm{t}} = \lceil \frac{N_{l,\min}^{\mathrm{t}}}{N_{\mathrm{sa}}} \rceil, \forall l \in \mathcal{L}_n^{\mathrm{t}}$. It is assumed to be feasible to use $M/2$ subarrays to serve all the links in $\mathcal{L}_n^{\mathrm{t}}$. For the receiving links of node n, the subarrays are equally allocated among them: $A_l^{\mathrm{r}} = \lfloor \frac{M}{2|\mathcal{L}_n^{\mathrm{r}}|} \rfloor, \forall l \in \mathcal{L}_n^{\mathrm{r}}$.

D. Bottleneck Structure Construction

To quantitatively determine the relationship between link resources and network saturation throughput expressed in equation (3), a bottleneck structure $\mathcal{G} = \langle \mathcal{V}, \mathcal{E} \rangle$ (a DAG) is constructed, which lies at the heart of bottleneck theory [10]. The vertex set $\mathcal{V}$ in the bottleneck structure consists of all the bottleneck links and flows in the network, while the edge set $\mathcal{E}$ comprises of the directed edges between bottleneck links and flows. The bottleneck links are identified based on max-min fairness by the GradientGraph algorithm in [10]. Let $(\mathrm{l}_m, \mathrm{f}_n)$ and $(\mathrm{f}_n, \mathrm{l}_m)$ denote the edge from link m to flow n, and the edge from flow n to link m, as shown in Fig. 3. The existence of directed edges specifies the impact of the former vertex to the latter one.

Given a certain link resource planning result and flow distribution, two key results are obtained by the construction of bottleneck structures. First, the network saturation throughput is obtained by taking the sum of each flow's saturation rate, e.g., denoted by $(r_1, ..., r_5)$ as shown in Fig. 3. The flow saturation rates are computed along with the construction of a bottleneck structure. Second, the gradients $\partial r_f / \partial C_l$ are computed using the ForwardGrad algorithm [10] based on the constructed bottleneck structure, which quantifies how the capacity increase of link l impacts flow f's saturation rate. For instance, the gradients with respect to C_2 are obtained in Fig. 3. In this work, the bottleneck gradient $\mathrm{grad}(l)$ is designed as a critical metric to capture how the capacity increase of link l impacts network saturation throughput, expressed by $\mathrm{grad}(l) = \partial T / \partial c_l = \partial(\sum_{f \in \mathcal{F}} r_f)/\partial c_l$. Following the above definition, the capacity increase of those links with larger positive bottleneck gradients has a greater boosting impact on the network saturation throughput.

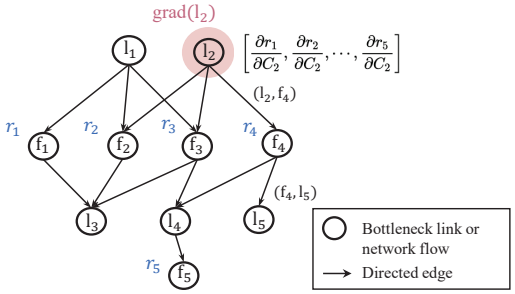


Fig. 3. The illustration of a bottleneck structure.

E. Subband and Power Planning

The bottleneck links are first sorted in a descending direction based on the bottleneck gradients defined in Section III-D. The top Q bottleneck links with available subbands are selected (satisfying constraint (6)), denoted by $\mathcal{L}_{\mathrm{G}}$. Since the capacity increase of these links has greater contribution to boosting network saturation throughput than other links, more subbands should be allocated to them. Therefore, for each link in $\mathcal{L}_{\mathrm{G}}$, greedy subband allocation is conducted where the subband with the largest SINR is allocated to it. Next, a new subband allocation matrix $\mathbf{B}$ is generated. With fixed $b_{l,k}$ in $\mathbf{B}$, the power allocation problem is formulated to maximize the sum capacities of links in $\mathcal{L}_{\mathrm{G}}$

Problem 1 (P1):

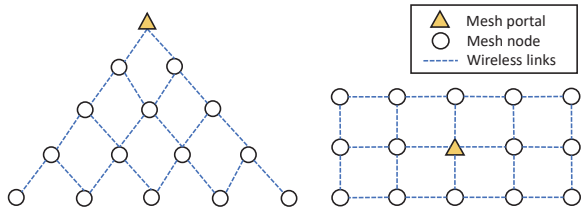
$$\max_{\mathbf{P}} \quad \sum_{l \in \mathcal{L}_{\mathrm{G}}} \sum_{k \in \mathcal{K}} b_{l,k} \log_2 [1 + \gamma_{l,k}], \quad (10)$$

$$\textbf{s.t.} : (5), (7), (8). \quad (11)$$

P1 is a classic non-convex problem, where Difference of Convex (DC) programming [11] can be adopted to obtain a local optimum. The key idea is transforming non-convex functions into the difference of two convex (or concave) functions. In P1, the objective function in (10) and constraint (5) are non-convex. Let $f_{l,k}(\mathbf{P}) = \log_2\left(\sum_{m \in \mathcal{L}} p_{m,k} |g_{m,l,k}^{\mathrm{eff}}|^2 + P_{\mathrm{N}}\right)$, where $g_{l,l,k}^{\mathrm{eff}} = h_{l,k}^{\mathrm{eff}}$. Also, let $u_{l,k}(\mathbf{P}) = \log_2\left(\sum_{m \in \mathcal{L}\setminus\{l\}} p_{m,k} |g_{m,l,k}^{\mathrm{eff}}|^2 + P_{\mathrm{N}}\right)$, and $v_{l,k}(\mathbf{P}) = \log_2\left(p_{l,k} |h_{l,k}^{\mathrm{eff}}|^2\right)$. The above three functions are all concave functions. Therefore, the objective function in (10) is equivalently transformed into the difference of two concave functions, which is $\sum_{l \in \mathcal{L}_{\mathrm{G}}} \sum_{k \in \mathcal{K}} b_{l,k} [f_{l,k}(\mathbf{P}) - u_{l,k}(\mathbf{P})]$, and similarly the constraint (5) is transformed into

$$b_{l,k} [v_{l,k}(\mathbf{P}) - u_{l,k}(\mathbf{P})] \geq b_{l,k} \log_2 \gamma_{\mathrm{th}}, \forall l \in \mathcal{L}, k \in \mathcal{K}. \quad (12)$$

Authorized licensed use limited to: University of Edinburgh. Downloaded on October 18,2026 at 20:09:29 UTC from IEEE Xplore. Restrictions apply.



(a) Diamond topology (b) Grid topology

Fig. 4. Network topologies.

Based on the transformation, P1 is solved by the existing method, i.e., successive convex approximation (SCA) as stated in [11].

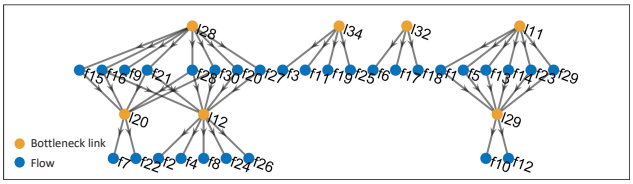
F. Overall Algorithm

The heuristic algorithm based on the framework in Section III-B is designed. Before iterations, the initial link planning result is obtained by conducting subarray allocation as in Section III-C, randomly allocating each link with one subband, and equally allocating power. The initial network saturation throughput is obtained by constructing the bottleneck structure given the initial planning result. Then, the iterative process starts with three key steps: (1) Based on the constructed bottleneck structure, bottleneck gradients are computed for all the bottleneck links to determine $\mathcal{L}_{\mathrm{G}}$ as in Section III-D; (2) The subband and power planning is conducted to boost capacities of links with large bottleneck gradients in $\mathcal{L}_{\mathrm{G}}$ as in Section III-E; (3) Based on the new link resource planning result, a new bottleneck structure is constructed as in Section III-D. The iterative process continues until the gap of network saturation throughput in two consecutive iterations is smaller than the convergence tolerance value, thus obtaining the optimized link resource planning result.

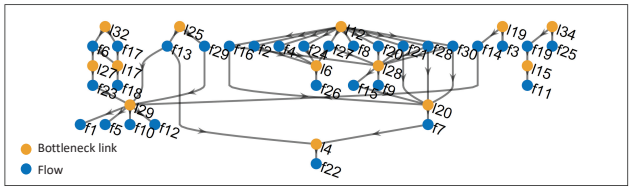
IV. Performance Evaluation

A. Simulation Set-up

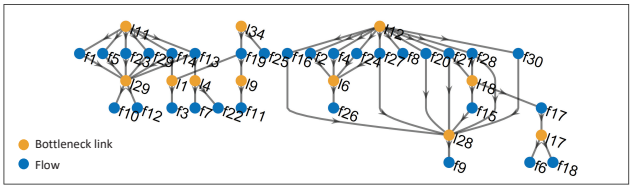
We consider a FDD-based THz mesh backhaul network with $K = 20$ subbands spanning from 100 GHz to 300 GHz. Each subband occupies the bandwidth of 10 GHz. As shown in Fig. 1, both the mesh portal and mesh nodes are deployed with the total transmit power P_n of 36 dBm and the total number of subarrays A_n of 32. Each subarray contains 2 antennas ($N_{\mathrm{sa}} = 2$). The channel model parameters follow [9]. The noise power spectrum density is assumed as -168 dBm/Hz. Two typical backhaul topologies with 15 nodes, diamond and grid topology, are considered, as shown in Fig. 4. The number of mesh nodes is fixed as 15. Link distance is uniformly distributed between 50 and 80m. The source-destination pair of each flow is randomly selected among all the network nodes. Other parameters in the simulation are as follows: the beam gain ratio $\beta = 0.25$; SINR threshold for each subband $\gamma_{\mathrm{th}} = 20$ dB; $Q = 5$ for subband and power allocation; the convergence tolerance $\epsilon = 0.01$ (Tbps); 3 dB antenna gain is added. To demonstrate the effectiveness of our heuristic algorithm named the bottleneck theory-based link resource planning (termed as BT-based planning in this section), two



(a) BT-based planning



(b) Random planning



(c) TL-based planning

Fig. 5. The comparison of bottleneck structures.

baseline methods are considered: random planning and traffic-load-based (TL-based) planning. In random planning, the mesh portal randomly allocates subbands to each link for each mesh node. In TL-based planning, links are sorted by their traffic loads (i.e., the number of flows) in subband and power planning [14], instead of bottleneck gradients. The transmit power is allocated such that the sum of link capacities is maximized in both cases.

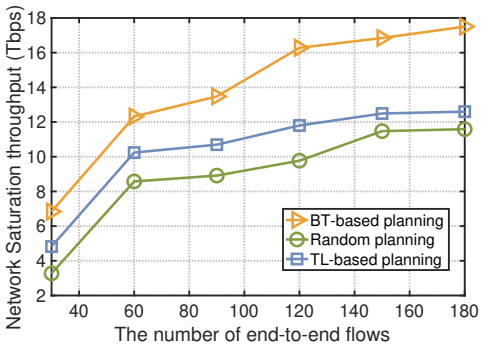
B. Comparison of Bottleneck Structures

As shown in Fig. 5, the bottleneck structures are constructed given the ultimate resource planning results of three methods, with grid topology and 30 end-to-end flows. As proved in [1], the smaller the depth of bottleneck structure is (i.e., the longest length of a directed path), the better the network congestion performance is. BT-based planning produces the flattest bottleneck structure with the depth as 3, and the fewest bottleneck links (colored in yellow), which means the interactions among bottleneck links are much less complicated than the other two methods.

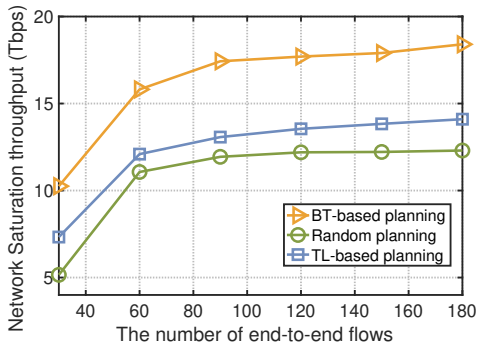
C. Network Saturation Throughput

As shown in Fig. 6(a) and 6(b), network saturation throughput with various numbers of end-to-end flows is simulated for two topologies. BT-based planning results in a much higher network saturation throughput than the other two methods when the flow number varies from 30 to 180. It outperforms the TL-based planning by 20.30% - 41.81% for diamond topology, and 29.44% - 39.91% for grid topology. It is observed that the network saturation throughput achieved by BT-based planning in grid topology is larger than that in diamond topology by $0.90 - 3.95$ Tbps. As the number of

Authorized licensed use limited to: University of Edinburgh. Downloaded on October 18,2026 at 20:09:29 UTC from IEEE Xplore. Restrictions apply.



(a) Diamond topology



(b) Grid topology

Fig. 6. Network saturation throughput with various number of flows.

flows increases, the edge of BT-based planning over the others becomes more significant.

Apart from network saturation throughput, the maximum flow completion time is evaluated for two topologies with 60 flows, which characterizes the longest time it takes for one flow to finish transmitting its data. The amount of traffic data for each flow is set as 1T bits. As shown in Fig. 7, the maximum flow completion time obtained by BT-based planning is smaller by around 6.04% - 9.44% compared with TL-based planning, and by 40.44% - 46.63% compared with random planning. All three methods result in the larger maximum flow completion time for grid topology than that for diamond topology.

V. Conclusion

A heuristic link resource planning algorithm based on the bottleneck theory was designed, to boost capacity for 6G THz mesh networks. Via constructing the bottleneck structure, the relationship between link resources and network capacity was obtained, and the bottleneck gradients were computed, based on which an iterative link resource planning process was conducted. It is the first work that adapts the bottleneck theory for wireless networks by considering the peculiarities of THz mesh networking.

Several interesting topics need to be further investigated. First, the network capacity gain achieved by load balancing as compared to our designed approach needs to be evaluated. Second, the approach used in this work cannot be directly applied to a general wireless network with complicated interference patterns. How to resolve this problem is subject to future work.

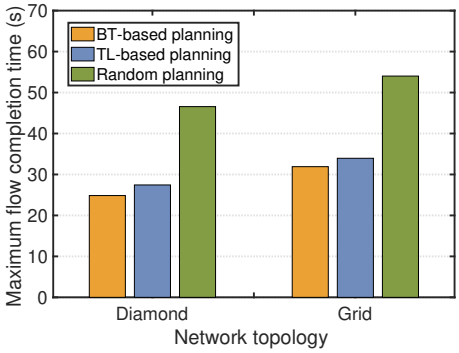


Fig. 7. Maximum flow completion time in two network topologies.

References

[1] J. Ros-Giralt, A. Bohara, S. Yellamraju, M. H. Langston, R. Lethin, Y. Jiang, L. Tassiulas, J. Li, Y. Tan, and M. Veeraraghavan, "On the bottleneck structure of congestion-controlled networks," in *Proc. ACM SIGMETRICS*, Phoenix, USA, Dec. 2019, pp. 1–31.

[2] I. F. Akyildiz, C. Han, Z. Hu, S. Nie, and J. M. Jornet, "Terahertz band communication: An old problem revisited and research directions for the next decade," *IEEE Trans. on Commun.*, vol. 70, no. 6, pp. 4250–4285, Jun. 2022.

[3] M. Yu, A. Tang, X. Wang, and C. Han, "Joint scheduling and power allocation for 6g terahertz mesh networks," in *Proc. Int. Conf. Comp., Netw. and Commun. (ICNC)*, Big Island, HI, USA, Feb. 2020, pp. 631–635.

[4] M. Zafer and E. Modiano, "Optimal rate control for delay-constrained data transmission over a wireless channel," *IEEE Trans. Inf. Theory*, vol. 54, no. 9, pp. 4020–4039, Sep. 2008.

[5] Chai Keong Toh, Anh-Ngoc Le, and You-Ze Cho, "Load balanced routing protocols for ad hoc mobile wireless networks," *IEEE Commun. Mag.*, vol. 47, no. 8, pp. 78–84, Aug. 2009.

[6] J. Ros-Giralt, N. Amsel, S. Yellamraju, J. Ezick, R. Lethin, Y. Jiang, A. Feng, L. Tassiulas, Z. Wu, M. Y. Teh, and K. Bergman, "Designing data center networks using bottleneck structures," in *Proc. ACM SIGCOMM*, Virtual Event USA, Aug. 2021, pp. 319–348.

[7] B. Zhai, A. Tang, C. Huang, C. Han, and X. Wang, "Antenna subarray management for hybrid beamforming in millimeter-Wave mesh backhaul networks," *Nano Commun. Netw.*, vol. 19, pp. 92–101, Mar. 2019.

[8] T. Wang, S. Chen, Y. Zhu, A. Tang, and X. Wang, "Linkslice: Fine-grained network slice enforcement based on deep reinforcement learning," *IEEE J. Sel. Areas Commun.*, vol. 40, no. 8, pp. 2378–2394, 2022.

[9] B. Zhai, A. Tang, C. Peng, and X. Wang, "SS-OFDMA: Spatial-spread orthogonal frequency division multiple access for terahertz networks," *IEEE J. Sel. Areas Commun.*, vol. 39, no. 6, pp. 1678–1692, 2021.

[10] J. Ros-Giralt, N. Amsel, S. Yellamraju, J. Ezick, R. Lethin, Y. Jiang, A. Feng, and L. Tassiulas, "A quantitative theory of bottleneck structures for data networks," *arXiv preprint arVix:2210.03534*, Oct. 2022.

[11] C. Kai, H. Li, L. Xu, Y. Li, and T. Jiang, "Joint subcarrier assignment with power allocation for sum rate maximization of D2D communications in wireless cellular networks," *IEEE Trans. Veh. Techn.*, vol. 68, no. 5, pp. 4748–4759, May 2019.

[12] Z. Wei, D. W. K. Ng, and J. Yuan, "Noma for hybrid mmwave communication systems with beamwidth control," *IEEE J. Sel. Topics Signal Process.*, vol. 13, no. 3, pp. 567–583, Jun. 2019.

[13] Q. Xia and J. M. Jornet, "Multi-hop relaying distribution strategies for terahertz-band communication networks: A cross-layer analysis," *IEEE Trans. on Wireless Commun.*, vol. 21, no. 7, pp. 5075–5089, Jul. 2022.

[14] W. Ni, I. B. Collings, X. Wang, and R. P. Liu, "Multi-hop point-to-point FDD wireless backhaul for mobile small cells," *IEEE Wireless Commun.*, vol. 21, no. 4, pp. 88–96, Aug. 2014.

Authorized licensed use limited to: University of Edinburgh. Downloaded on October 18,2026 at 20:09:29 UTC from IEEE Xplore. Restrictions apply.